Spectroscopy and electronic structure of jet-cooled NiPd and PdPt

Scott Taylor, Eileen M. Spain, and Michael D. Morse
Department of Chemistry, University of Utah, Salt Lake City, Utah 84112

(Received 6 September 1989; accepted 10 November 1989)

Resonant two-photon ionization spectroscopy of jet-cooled NiPd and PdPt has revealed a dense vibronic spectrum for NiPd and a much more sparse spectrum for PdPt. Four vibrational progressions have been identified for NiPd, and three have been located for PdPt. High resolution investigations of NiPd have established a ground state bond length of $r_0'' = 2.242 \pm 0.005$ Å with $\Omega'' = 2$. The observed spectra have been used to bracket the ionization potentials, giving IP(NiPd) $= 7.18 \pm 0.76$ eV and IP(PdPt) $= 8.27 \pm 0.38$ eV. In contrast to previous work on Ni_2, NiPt, and Pt_2, no abrupt onset of rapid predissociation is observed for either NiPd or PdPt. A discussion of this result in terms of the expected potential energy curves for the palladium-containing diatomics is presented, which when combined with the frequencies of the highest energy vibronic bands observed yields estimates of $D_0(\text{NiPd}) \approx 1.46$ eV and $D_0(\text{PdPt}) \approx 1.98$ eV. The lack of observable vibronic transitions in Pd_2 above 11 375 cm^{-1} places $D_0(Pd_2)$ below 1.41 eV, in agreement with Knudsen effusion mass spectrometry. Finally a comparison of the platinum group dimers and the coinage metal dimers is given, demonstrating the increasing importance of *d*-orbital contributions to the bonding in the platinum group dimers as one moves down the periodic table. The anomalous behavior of the palladium-containing diatomics is also discussed in terms of the highly stable $4d^{10}5s^0$, $^1S_0$ ground state of atomic palladium.

I. INTRODUCTION

The spectroscopy of transition metal dimers is a rich source of fundamental information on the nature of the metal–metal chemical bond and the role played by the *d* orbitals in that bond. As the smallest molecules containing chemical bonds between transition metal atoms, the dimers represent basic units which must be understood before detailed progress in understanding larger transition metal clusters can be made. Given the intense experimental[1–4] and theoretical[5–8] activity currently directed toward understanding the transition metal clusters, spectroscopic work on the diatomic metals provides the foundation of knowledge upon which an understanding of larger systems can be erected.

The platinum group metal dimers (Ni_2, Pd_2, Pt_2, NiPd, NiPt, and PdPt) provide an excellent starting point for a spectroscopic journey into the realm of the open *d*-subshell transition metal dimers. With the exception of palladium, these elements lack only one electron of having a closed *d* subshell, and therefore may be expected to have a simpler electronic structure than might be found among dimers formed from transition metals nearer to the center of the periodic table. In addition, the *d*-electron contributions to the chemical bonding in the platinum group dimers may be readily evaluated by comparisons to the relatively well-known coinage metal dimers. In the coinage metals (Cu, Ag, and Au), the atomic ground state is $d^{10}s^1$, ^2S, and the first excited state (d^9s^2, ^2D for Cu and Au; $d^{10}p^1$, ^2P for Ag) lies quite high in energy (1.49, 3.74, and 1.14 eV for Cu, Ag, and Au, respectively).[9] As a result, the ground states of the coinage metal dimers are well described as $d_A^{10}d_B^{10}\sigma^2$, $^1\Sigma^+$ states without significant *d*-electron contributions to the chemical bonding. Substantial differences between a platinum group dimer and the corresponding coinage metal diatomic may then be attributed to the effects of the open *d* subshell on the chemical bond.

Despite the expectation of relatively simple electronic structure in the platinum group dimers, theoretical calculations on Ni_2,[10–12] Pd_2,[13–15] and Pt_2,[15,16] demonstrate that the electronic structure of these species is actually quite complex. It is simple only in comparison to what is expected deeper into the transition metal series, where the density of low-lying electronic states becomes even more extreme. With this in mind, the platinum group dimers are a superb proving ground for testing theoretical methods of calculating the complicated open *d*-subshell transition metals. Their electronic structure is sufficiently complex to be a reasonable test of the methods, but is substantially more tractable than what is lurking deeper in the transition metal jungle.

To date, the Ni_2,[17] Pt_2,[18] and NiPt[19] molecules have been investigated using the technique of resonant two-photon ionization spectroscopy. In this paper, a study of the remaining platinum group dimers, NiPd, PdPt, and Pd_2, is presented. This completes the initial survey of the platinum group dimers by the resonant two-photon ionization spectroscopic method. As will become evident in Sec. III, the chemical bonding in these palladium-containing species is somewhat different from what is found for Ni_2, NiPt, and Pt_2, primarily because of the high stability of the $4d^{10}5s^0$, ^1S ground state of atomic palladium. For this reason it is appropriate to consider the palladium-containing species separately from Ni_2, NiPt, and Pt_2.

Section II of this paper describes the experimental aspects of this work, including the methods employed to prepare targets for the mixed dimer studies. Results of both low- and high-resolution investigations are presented in Sec. III. These findings are discussed in Sec. IV, where comparisons to the remaining platinum group and coinage metal dimers

 0021-9606/90/052710-11$03.00

are made. Section V then concludes the paper with a summary of the most important results.

II. EXPERIMENTAL

The molecular beam apparatus employed for these investigations is essentially identical to that used in previous studies of the diatomic transition metals Pt_2,[18] NiPt,[19] NiCu,[20] and CuAg.[21] A pulsed supersonic beam of the dimer of interest is produced by laser vaporization of a suitable target material (see below) in the throat of a pulsed supersonic nozzle using the second harmonic light of a Q-switched Nd:YAG laser (532 nm, 25–50 mJ/pulse, focused to a diameter of approximately 0.5 mm). The vaporization laser is timed to fire at the peak density of helium carrier gas, which is pulsed over the target by a magnetically operated double solenoid valve. The high pressure of helium (8 atm stagnation pressure) insures sufficient three-body collisions in the 2 mm diameter nozzle throat to quench the plasma and stabilize dimers and higher metal clusters. As described for NiPt,[19] formation of diatomic NiPd, PdPt, and larger clusters is facilitated by attaching a faceplate and extender to the nozzle. Following this cluster agglomeration/thermalization region, a final expansion from a 1 mm diameter orifice into vacuum cools the metal dimers to a few degrees Kelvin. The supersonic jet is then skimmed, and the central portion of the jet is admitted into the ionization region of a reflectron-type time-of-flight mass spectrometer.

Ionization of the clusters is accomplished by a resonant two-photon ionization process, following which the ions are accelerated up a 0.9 m flight tube. A set of electrodes mounted at the apex of the flight tube reflects the ions through an 18° angle down a second flight tube, where detection is achieved using a dual microchannel plate assembly. The signal is preamplified, digitized, and signal averaged. The entire experiment operates under the control of a DEC 11/73 microcomputer, and is repeated at a rate of 10 Hz. A more complete description of the apparatus (including a scale drawing) and data collection methods is provided in Ref. 22.

Resonant two-photon ionization spectra of NiPd and PdPt were obtained using a scanning dye laser pumped by the second or third harmonic radiation of a Q-switched Nd:YAG laser to excite the molecule of interest. Following excitation, photoionization was achieved by subjecting the excited molecules to the output of an excimer laser operating on the ArF (193 nm, 6.42 eV) or F_2 (157 nm, 7.9 eV) transition. Excited state lifetimes were determined by monitoring the ion signal as a function of the time delay between the excitation and the ionization pulses. High-resolution spectra of NiPd were recorded using an intracavity etalon to narrow the output of the dye laser to approximately 0.03 cm^{-1}, and pressure scanning the oscillator cavity from 0 to 1 atm using SF_6. Absolute line positions were obtained by simultaneously monitoring the absorption spectrum of gaseous I_2 and calibrating each scan using the precisely known I_2 absorption lines.[23,24] In the course of this investigation the dye laser was operated on coumarin 540A; rhodamines 590, 610, and 640; DCM; and LDS dyes 698, 750, 751, 765, 821, 867, and 925 (all obtained from Exciton).

The primary experimental problem which had to be solved to investigate the mixed transition metal dimers concerned the metal source. For the study of NiPt[19] and PdPt (as reported here), a commercially prepared equimolar alloy of nickel, palladium, and platinum (Alfa, $1.0 \times 25 \times 25$ mm^3, 99.9% purity) was purchased. Laser vaporization of this target, using a rotating disk vaporization mount similar to that described in Ref. 25, was found to generate large quantities of Pt_2, NiPt, and Ni_2, and adequate quantities of PdPt. The amounts of Pd_2 and NiPd produced by vaporization of the equimolar alloy, however, were insufficient for spectroscopic investigations. Spectroscopic studies of Pd_2 were undertaken using a pure palladium foil, which generated copious amounts of Pd_2. Spectroscopic investigations of NiPd, however, required a separate mixed metal target. To produce this target, powdered palladium (Alfa, 99.95% purity, 1.0–1.5 μm particles) and powdered nickel (Alfa, 99.9% purity, 2.5–3.0 μm particles) were mixed in an equimolar ratio and were pressed under 25 000 psi to form a pellet. The consistency of the resulting pellet was not very good, however, and it was not useful for laser vaporization because it crumbled readily. To improve the structural integrity of the metal target, the pellet was transferred to an electric arc melting furnace where it was placed on a water-cooled copper cathode. An electric arc was then ignited between three tungsten–thorium anodes and the sample, under an inert atmosphere of argon. The current was slowly increased until the sample melted, after which the current was discontinued and the sample was allowed to cool. The nugget produced by this process was then placed in a 1 in. diameter tungsten carbide die and pressed into the shape of a disk by 100 tons of force. Finally, the 1.5 mm thick by 10 mm diameter disk was polished to flatness with a diamond polishing wheel. The resulting metal target provided an excellent, stable source of NiPd molecules.

III. RESULTS

A. Mass spectra and diatomic abundances

As mentioned in Sec. II, laser vaporization of an equimolar mix of nickel, palladium, and platinum resulted in the formation of diatomic species with intensities $Pt_2 > NiPt > Ni_2 > PdPt \gg NiPd, Pd_2$. Indeed, the intensities of NiPd and Pd_2 produced from the triple mixture source were too low to be of use. This intensity pattern for the various diatomic molecules is probably *not* due to preferential vaporization of platinum over nickel over palladium, since the melting and boiling points of the pure metals fall in the order Ni (MP 1728 K, BP 3110 K)[26] < Pd (MP 1823 K, BP 3400 K)[26] < Pt (MP 2043 K, BP 4100 K).[26] Instead, we propose that the observed pattern of intensities is controlled by the stabilities of the individual diatomic molecules. From previous work it is known that the bond strengths of the nickel and platinum containing dimers fall in the order $D_0(Pt_2) = 3.14 \pm 0.02$ eV[18] $> D_0(NiPt) = 2.798 \pm 0.003$ eV[19] $> D_0(Ni_2) = 2.068 \pm 0.010$ eV.[17] Assuming that the stabilities of the diatomic molecules control the abundance pattern obtained from the laser vaporization source, this pattern of bond strengths predicts the intensity distribution $Pt_2 > NiPt > Ni_2$, as is observed.

We do not mean to suggest that the laser vaporization source produces a dynamic equilibrium between atomic and diatomic species, as is obtained in a Knudsen effusion mass spectrometric study. This cannot be correct, since replacement of the triple mixture target with a pure palladium target leads to a vast increase in the $[Pd_2]/[Pd]^2$ signal. The laser vaporization source is far removed from thermodynamic equilibrium, and the pattern of intensities is controlled by kinetics rather than thermodynamics. The rate of production of Pd_2, for example, is governed by the values of k_1, k_{-1}, and k_2 in the mechanism:

$$Pd + Pd \underset{k_{-1}}{\overset{k_1}{\rightleftarrows}} Pd_2^* \quad \text{(bimolecular association)}, \tag{3.1}$$

$$Pd_2^* + He \xrightarrow{k_2} Pd_2 \quad \text{(stabilization)}. \tag{3.2}$$

These constants are independent of the composition of the disk which is vaporized, so the rate of Pd_2 formation should be roughly independent of the composition of the target disk, except for the obvious dependence on $[Pd]^2$. Nevertheless, we still observe a vast increase in $[Pd_2]/[Pd]^2$ signal when the triple mixture source is replaced with a pure palladium target.

We believe that the rate of Pd_2 formation does follow mechanism (3.1) and (3.2), even when the triple mixture source is used. However, displacement reactions such as

$$Pt + Pd_2 \rightarrow PdPt + Pd \tag{3.3}$$

become possible when more than one metal is vaporized. These subsequent displacement reactions will always favor production of the more stable diatomic molecule, resulting in an intensity distribution indicative of the dimer stabilities.

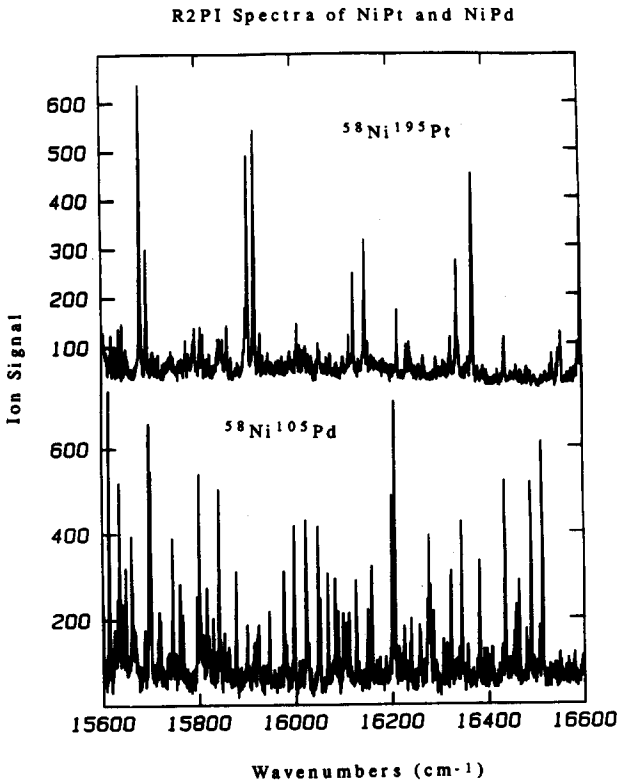

FIG. 1. Resonant two-photon ionization spectra of $^{58}Ni^{105}Pd$ (lower panel) and $^{58}Ni^{195}Pt$ (upper panel) over the frequency range from 15 600 to 16 600 cm^{-1}. In this spectral range a much greater density of vibronic features is present in the spectrum of NiPd as compared to NiPt. This suggests a smaller splitting of the *d* orbitals into bonding and antibonding pairs in NiPd as compared to NiPt.

B. Vibronic spectra of NiPd

Low-resolution scans of the resonant two-photon ionization spectrum of NiPd reveal a large number of vibronic bands throughout the range 12 150 to 18 300 cm^{-1}. The red portion of the spectrum (below 15 000 cm^{-1}) exhibits a relatively sparse density of optically accessible excited states, averaging approximately one vibronic band every 50 cm^{-1}. From 15 000 to 18 000 cm^{-1}, however, the density of vibronic bands is much higher, averaging one band every 17 cm^{-1}. A portion of this high density region is shown in Fig. 1, where a spectrum of NiPt in the same frequency range is provided for comparison. No definite vibronic features are observed to the blue of 18 300 cm^{-1} or to the red of 12 150 cm^{-1}.

The high density of vibronic features in NiPd as compared to NiPt suggests that *d*-electron contributions to the chemical bonding in NiPd are less significant than in NiPt. This suggestion is based on the idea that as the *d*-orbital contributions to the chemical bonding become more important, the *d* orbitals split into bonding and antibonding pairs. As the magnitude of this splitting increases, the electronic states associated with different arrangements of electrons in the *d* orbitals spread over a broader range in energy, resulting in a less congested spectrum. The increased spectral congestion found for NiPd over NiPt is therefore an indicator of decreased *d*-orbital bonding contributions in NiPd as compared to NiPt. In this respect the vibronic spectrum of NiPd is reminiscent of that found for Ni_2,[17] although the congestion in NiPd is less severe than in Ni_2, and does not persist so far to the red. These considerations would tend to place the *d*-orbital contribution to the bonding in NiPd at an intermediate value, between that found for Ni_2[17] and NiPt.[19]

The densely packed vibronic features in the spectrum displayed in Fig. 1 have not readily succumbed to vibrational analysis. Further to the red, however, three progressions have been tentatively identified. In addition, one vibrational progression containing the strongest features in the spectrum has been identified further to the blue. Despite some uncertainty in these assignments, the bands have been fitted to vibronic progressions, as indicated in Table I. The deviations between calculated and observed band positions are generally small, suggesting acceptable assignments. Unfortunately, the observed isotope shifts are erratic and are of little use in establishing absolute vibrational numberings in these band systems. Undoubtedly numerous perturbations are present, resulting in small random shifts of the vibronic levels. Variations in these shifts between the various isotopic modifications are significant, but it is generally still possible to correlate particular vibronic features between isotopic modifications. In this respect NiPd remains slightly less problematic than Ni_2,[17] where correlation of vibronic features between isotopic forms usually proved to be impossible.

TABLE I. Band systems of NiPd.[a]

System	Band[b]	ν (^{58}Ni^{105}Pd)	$\nu_{obs} - \nu_{calc}$ [b]	Isotope shift[c] ^{58}Ni^{108}Pd	Isotope shift[c] ^{60}Ni^{106}Pd
A	0–0	12 386.96	0.84	1.85	6.69
	1–0	12 585.81	−0.96	4.17	15.71
	2–0	12 783.97	−1.32	4.94	11.94
	3–0	12 983.06	1.37	5.21	13.86
	4–0	13 176.86	0.89	5.55	14.25
	5–0	13 367.31	−0.81	8.29	16.39
B	0–0	12 873.53	−0.20	d	d
	1–0	13 084.62	0.52	1.79	8.02
	2–0	13 289.10	−0.16	4.99	13.29
	3–0	13 488.44	−0.78	4.14	14.70
	4–0	13 684.98	1.01	6.85	18.72
	5–0	13 873.04	−0.48	9.58	22.44
	6–0	14 057.94	0.08	11.60	27.75
C	0–0	13 551.43	1.30	d	d
	1–0	13 760.41	−2.33	6.54	16.69
	2–0	13 970.13	−0.80	8.70	21.13
	3–0	14 178.07	3.39	9.53	25.27
	4–0	14 372.43	−1.56	d	d
D	0–0	17 103.65	0.77	d	d
	1–0	17 270.55	−0.62	d	d
	2–0	17 435.42	−1.73	d	d
	3–0	17 602.08	1.27	d	d
	4–0	17 763.49	1.33	d	d
	5–0	17 920.19	−1.00	d	d

[a] All reported quantities are given in wave numbers (cm^{-1}). Absolute band frequencies may be in error by $\pm 10\ cm^{-1}$; the relative error is probably below $\pm 2\ cm^{-1}$.

[b] Each band system was fitted to the formula $\nu = \nu_{00} + \omega_e' v' - \omega_e' x_e' (v'^2 + v')$. Although in most cases the first observed band is certainly not the $v' = 0 \leftarrow v'' = 0$ transition, this assignment was adopted for purposes of fitting the data. With this procedure we obtain ν_{00}, ω_e', and $\omega_e' x_e'$ for ^{58}Ni^{105}Pd as follows, where the errors represent 1σ in the least-squares fit:
System A: $\nu_{00} = 12\ 386.12 \pm 1.35\ cm^{-1}$, $\omega_e' = 202.77 \pm 1.51\ cm^{-1}$, $\omega_e' x_e' = 1.06 \pm 0.24\ cm^{-1}$.
System B: $\nu_{00} = 12\ 873.72 \pm 0.65\ cm^{-1}$, $\omega_e' = 215.58 \pm 0.58\ cm^{-1}$, $\omega_e' x_e' = 2.60 \pm 0.08\ cm^{-1}$.
System C: $\nu_{00} = 13\ 550.13 \pm 3.10\ cm^{-1}$, $\omega_e' = 217.04 \pm 4.52\ cm^{-1}$, $\omega_e' x_e' = 2.22 \pm 0.88\ cm^{-1}$.
System D: $\nu_{00} = 17\ 102.88 \pm 1.51\ cm^{-1}$, $\omega_e' = 170.61 \pm 1.69\ cm^{-1}$, $\omega_e' x_e' = 1.16 \pm 0.27\ cm^{-1}$.

[c] Isotope shifts are defined as $\nu(^{58}Ni^{105}Pd) - \nu$ (isotopic modification).

[d] Data for isotope shifts are missing where bands were too weak to be observed, or where the density of vibronic features prevented a definite correlation of bands between isotopically different species (system D).

The observation of vibronic features as far to the red as 12 193 cm^{-1} (1.512 eV) using ArF ionizing radiation places the ionization potential of NiPd in the range $6.42 < IP(NiPd) < 7.93$ eV. On this basis we report $IP(NiPd) = 7.18 \pm 0.76$ eV.

C. Rotationally resolved spectra of NiPd

Four bands of NiPd were examined under high resolution (0.03 cm^{-1}). Three of these fell into regions where the iodine absorption spectrum[23,24] provided an excellent calibration, enabling precise line positions to be measured. Figures 2–4 display the rotationally resolved spectra of ^{58}Ni^{105}Pd for these three bands, along with simulated spectra. Evident in each of these scans is the immediate formation of a bandhead in the R branch, indicating a considerable lengthening of the NiPd bond upon electronic excitation. Each scan also shows a strong series of P-branch lines proceeding off to the red, and a Q branch which is initially strong, but which rapidly drops in intensity with increasing J. The rough equivalence of intensities in the P and R branches, and the rapid drop in Q-branch intensity with increasing J are characteristic of a $\Delta\Omega = 0$ band in Hund's case (c), as is surely the appropriate case for NiPd. Careful examination of the observed spectra and comparison to spectral simulations demonstrate that all of the rotationally resolved bands are $\Omega' = 2 \leftarrow \Omega'' = 2$ transitions.

Individual rotational line frequencies and their assignments are given in Table II for all three bands shown in Figs. 2–4. Each band has been fitted to the standard formula $\nu = \nu_0 + B'J'(J'+1) - B''J''(J''+1)$, and the resulting values of ν_0, B', and B_0'' are given in the footnotes to Table II. The linear least-squares fits reproduce the measured line frequencies extremely well, with the largest error being only 0.014 cm^{-1}. The average of the measured B_0'' values is $0.089\ 83 \pm 0.0004\ cm^{-1}$, giving a bond length of ground state NiPd of $r_0'' = 2.242 \pm 0.005$ Å. The bond lengths in

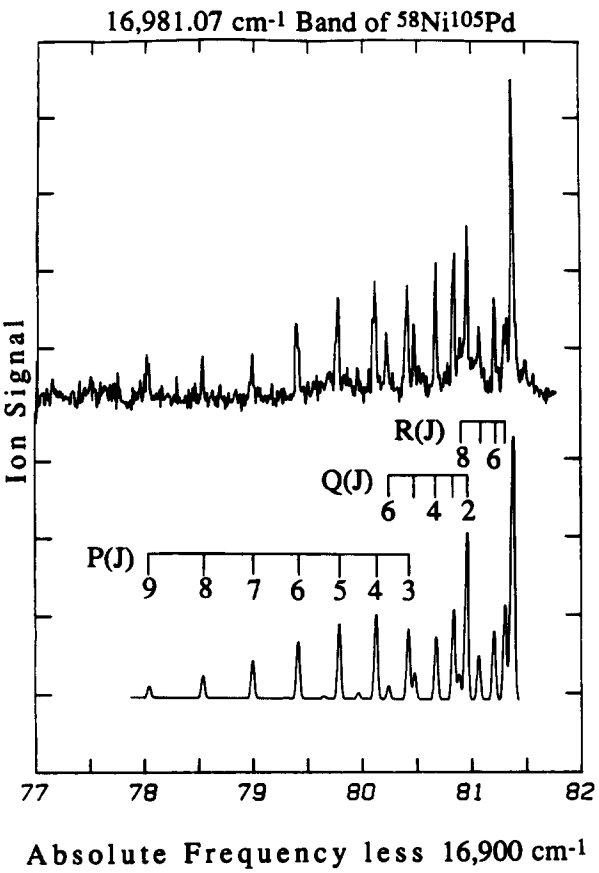

FIG. 2. High resolution spectrum of the 16 981.07 cm^{-1} band of $^{58}Ni^{105}Pd$. The upper trace was recorded by pressure scanning the oscillator cavity of a pulsed dye laser operating on rhodamine 610 (basic solution) using ArF radiation as the ionization source. The lower trace is a simulated spectrum for an $\Omega' = 2 \leftarrow \Omega'' = 2$ transition, with a rotational temperature of 3 K, a laser linewidth of 0.03 cm^{-1}, and with $B'' = 0.089\,43$ cm^{-1}, $B' = 0.069\,49$ cm^{-1}.

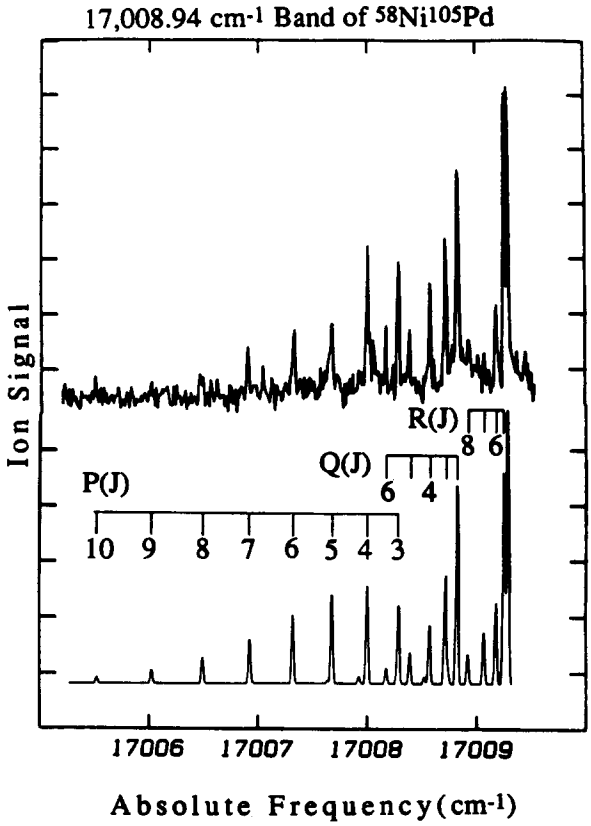

FIG. 3. High resolution spectrum of the 17 008.94 cm^{-1} band of $^{58}Ni^{105}Pd$, again obtained using a pulsed dye laser operating on rhodamine 610 (basic solution). The lower trace is a simulated spectrum with $\Omega' = \Omega'' = 2$, a rotational temperature of 3 K, a laser linewidth of 0.02 cm^{-1}, and with $B'' = 0.090\,00$ cm^{-1}, $B' = 0.071\,90$ cm^{-1}.

the excited states probed vary from $r' = 2.506$ Å to $r' = 2.583$ Å, demonstrating the large increase in bond length upon electronic excitation which was deduced from the immediate R-branch head.

D. Vibronic spectra of PdPt

A low-resolution investigation of PdPt, produced by laser vaporization of the equimolar NiPdPt source, produced a series of vibronic bands in the region from 16 800 to 22 500 cm^{-1}. From 16 800 to 19 000 cm^{-1} the density of observed transitions was extremely sparse as compared to what is observed for Ni_2,[17] NiPd, NiPt,[19] or Pt_2,[18] with an average spacing of 80 cm^{-1} between vibronic bands. Above 19 000 cm^{-1} the density of optical features increased somewhat, but never approached the density of transitions found for the other platinum group dimers.

Three regular vibronic progressions have been identified in the spectrum of PdPt, as listed in Table III. A portion of the spectrum is displayed in Fig. 5, where the A and B band systems are labeled. The density and regularity of the observed transitions is reminiscent of the spectra of Pt_2[18] in the region between 11 000 and 16 000 cm^{-1}, although the upper state vibrational frequencies in PdPt are much lower than in Pt_2. The observation of vibronic features as far to the red as 17 935 cm^{-1} (2.224 eV) using ArF (193 nm, 6.42 eV) ionization radiation places the ionization potential of PdPt below 8.65 eV, and the observation of transitions using F_2 (157 nm, 7.9 eV) radiation for the second, ionizing photon places the ionization potential above 7.9 eV. Accordingly, we report a value of 8.27 $\pm$ 0.38 eV for the ionization potential of PdPt.

E. Vibronic spectra of Pd_2

In the course of this work, the spectral region from 11 375 to 23 000 cm^{-1} has been scanned, and no transitions have been found in diatomic palladium. High temperature measurements of the $2Pd \rightleftarrows Pd_2$ equilibrium by Knudsen effusion mass spectrometry have provided a second-law value of $D_0(Pd_2) = 1.13 \pm 0.22$ eV,[27] and a reinvestigation of this equilibrium coupled with *ab initio* calculations has provided a third-law value of $D_0(Pd_2) = 1.03 \pm 0.16$ eV.[13] These estimates of the Pd_2 bond strength lie significantly lower in energy than the spectral regions we have investigated. We believe that spectroscopic transitions in Pd_2 certainly occur in the 11 375 to 23 00 cm^{-1} range, but efficient predissociation prevents their observation by the resonant two-photon ionization technique. Given the success in finding spectroscopic transitions in all of the remaining platinum group dimers,[17-19] this failure in the case of Pd_2 corroborates

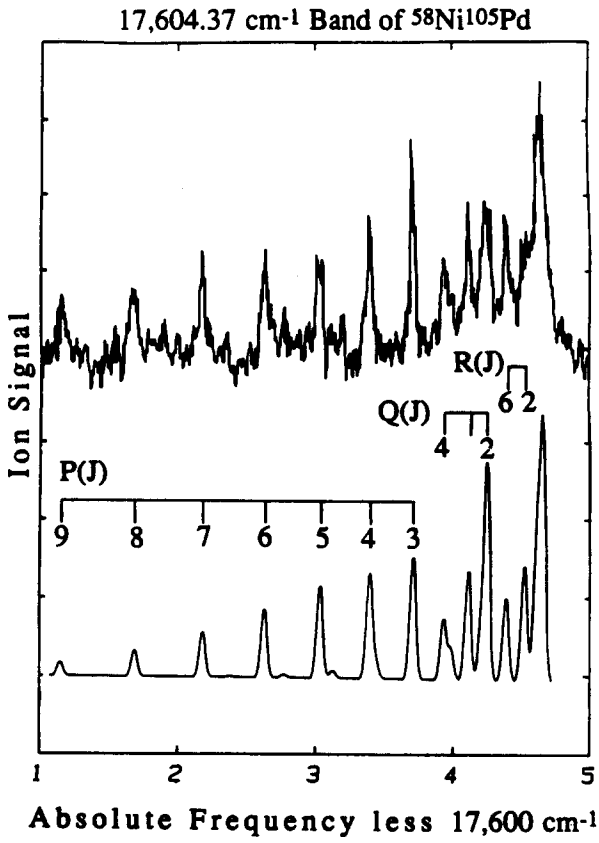

FIG. 4. High resolution spectrum of 17 604.37 cm^{-1} band of $^{58}Ni^{105}Pd$, obtained using a pulsed dye laser operating on rhodamine 590. The lower trace is a simulated spectrum with $\Omega' = \Omega'' = 2$, a rotational temperature of 3 K, a laser linewidth of 0.043 cm^{-1}, and with $B'' = 0.090\,06$ cm^{-1}, $B' = 0.067\,69$ cm^{-1}. This band is the most intense band in the spectrum of NiPd, and is the 3–0 band of system D as listed in Table I.

the low bond strength reported by Knudsen effusion mass spectrometry.[13,27]

F. Excited state lifetimes in NiPd and PdPt

In previous investigations of Ni_2[17] and NiPt,[19] an abrupt predissociation threshold was observed where the excited state lifetime suddenly dropped by a factor of 1000 as efficient predissociation set in. In Pt_2,[18] an abrupt predissociation onset was also observed, with a corresponding drop in excited state lifetime of a factor of 10. In all three cases it was argued that the sudden onset of efficient predissociation occurred as soon as the lowest dissociation threshold was exceeded, thereby permitting the bond strengths of Ni_2,[17] NiPt,[19] and Pt_2[18] to be measured to high precision, giving 2.068 ± 0.010, 2.798 ± 0.003, and 3.14 ± 0.02 eV, respectively. The crux of the argument was that these species possess hundreds of electronic states which are energetically accessible at the lowest dissociation limit, making the assumption of motion on a single Born–Oppenheimer potential surface untenable. Perturbations coupling the initially excited state to a dissociative potential energy surface then cause predissociation to occur as soon as it is energetically possible.

With the hope of making an analogous measurement of D_0 (NiPt) and D_0(PdPt), an extensive series of lifetime measurements were made on both molecules, using the method of time-delayed resonant two-photon ionization. The results of these measurements are shown in Figs. 6 and 7 for NiPd and PdPt, respectively. Although the measurements show a trend toward shorter lifetimes as the energy is increased for both species, neither molecule shows the abrupt drop in lifetime which was found for Ni_2,[17] NiPt,[19] and Pt_2.[18] As a result, no definitive values of D_0(NiPd) or D_0(PdPt) can be inferred from the lifetime data. Based on the highest frequency vibronic bands observed in each molecule, however, upper limits on the bond strengths may be tentatively derived as $D_0(\text{NiPd}) \leqslant 2.27$ eV and $D_0(\text{PdPt}) \leqslant 2.79$ eV. This inference assumes that more optically accessible states are present to higher energy, but cannot be observed by resonant two-photon ionization methods due to efficient predissociation in the excited electronic state.

IV. DISCUSSION

The results presented above demonstrate some striking differences between the palladium-containing platinum group dimers (NiPd, Pd_2, and PdPt) and the remaining platinum group dimers (Ni_2, NiPt, and Pt_2). Among these distinctions are the failure to observe sharp predissociation thresholds for NiPd and PdPt and the failure to observe any spectroscopic transitions in Pd_2 whatsoever. Ultimately both of these differences may be traced to the extraordinary stability of the $4d^{10}5s^0$, ^1S ground configuration of atomic palladium.

In the preceding article,[19] Fig. 6 presents a plot of the integrated density of electronic states $N(E)$ evaluated at the separated atom limit for Ni_2, NiPt, and Pt_2. The integrated density of electronic states $N(E)$ represents the number of distinct relativistic adiabatic potential curves [Hund's case (c) potential curves] which arise from separated atoms with total electronic energy less than E (measured relative to the energy of the separated ground state atoms). This plot of $N(E)$ vs E provides a simple means of estimating the number of potential energy curves which are available at a given energy. It may be readily constructed from the known atomic energy levels[9] and the Wigner–Witmer combination rules.[28] For Ni_2, NiPt, and Pt_2 this plot demonstrates that hundreds of potential energy curves arise within 2000 cm^{-1} of the lowest separated atom limit.[19] The analogous plots of $N(E)$ are provided for NiPd and PdPt in Fig. 8, where data for Ni_2 and NiPt are provided for comparison.

It is immediately obvious from Fig. 8 that very few molecular potential energy curves arise for Ni + Pd or Pd + Pt below a separated atom energy of 6000 cm^{-1}. This very low density of states below 6000 cm^{-1} occurs because below 6564 cm^{-1} the only accessible state of atomic palladium is the $4d^{10}5s^0$, $^1S_0$ ground state, which is nondegenerate.[9] The molecular states occurring below 6564 cm^{-1} for NiPd or PdPt arise simply by the splitting of the nickel or platinum atomic states in the axial field of a nondegenerate $^1S_0$ palladium atom. Above 6564 cm^{-1}, however, the filled $4d^{10}$ subshell of palladium may be cracked open, resulting in a vast increase in the number of molecular potential curves correlating to separated atom limits above this energy.

TABLE II. Rotational line positions and fitted values for $^{58}Ni^{105}Pd$.[a]

	16 981.07 cm^{-1} band[b]		17 008.94 cm^{-1} band[c]		17 604.37 cm^{-1} band[d,e]	
Assignment	Observed line position	Residual	Observed line position	Residual	Observed line position	Residual
$P(10)$	...	...	17 005.507	0.001	...	...
$P(9)$	16 978.019	− 0.004	6.026	0.001	17 601.148	0.007
$P(8)$	78.524	0.003	6.485	− 0.002	1.670	− 0.009
$P(7)$	78.980	0.001	6.907	0.014	2.170	− 0.002
$P(6)$	79.397	0.000	7.332	− 0.014	2.623	0.003
$P(5)$	79.777	0.002	7.677	− 0.002	3.020	− 0.004
$P(4)$	80.112	− 0.001	8.005	0.008	3.383	0.000
$P(3)$	80.410	− 0.002	8.293	− 0.005	3.701	0.004
$Q(6)$	80.222	− 0.009	8.181	0.000	...	...
$Q(5)$	80.474	0.004	8.398	0.000	...	...
$Q(4)$	80.667	− 0.002	8.581	0.002	3.933	0.008
$Q(3)$	80.833	0.004	8.725	0.001	4.103	− 0.001
$Q(2)$	80.950	0.002	8.832	0.000	4.231	− 0.007
$R(2)$	81.365	0.000	9.263	− 0.001	4.646	0.002
$R(3)$	R-branch head		9.293	− 0.006	R-branch head	
$R(4)$	81.365	0.001	R-branch head		R-branch head	
$R(5)$	81.300	− 0.004	R-branch head		R-branch head	
$R(6)$	81.201	− 0.002	9.187	0.000	4.378	− 0.002
$R(7)$	81.062	− 0.001	9.078	0.000	...	...
$R(8)$	80.889	0.006	8.934	0.002	...	...

[a] All numerical values are in wave numbers (cm^{-1}). Line positions were measured using the absorption spectrum of I_2 for calibration (Refs. 23 and 24), resulting in an accuracy of ± 0.01 cm^{-1} in absolute line positions. The line frequencies were the fitted to the formula $\nu = \nu_0 + B'J'(J'+1) - B''J''(J''+1)$. All uncertainties reported below represent one standard deviation (1σ) in the least-squares fit.

[b] Fitted constants: $\nu_0 = 16\,981.0679 \pm 0.0016$ cm^{-1}, $B_0'' = 0.089\,43 \pm 0.000\,08$ cm^{-1}, $B' = 0.069\,49 \pm 0.000\,08$ cm^{-1}, giving $r_0'' = 2.247 \pm 0.001$ Å, $r' = 2.549 \pm 0.002$ Å.

[c] Fitted constants: $\nu_0 = 17\,008.9410 \pm 0.0024$ cm^{-1}, $B_0'' = 0.090\,00 \pm 0.000\,12$ cm^{-1}, $B' = 0.071\,90 \pm 0.000\,13$ cm^{-1}, giving $r_0'' = 2.240 \pm 0.002$ Å, $r' = 2.506 \pm 0.002$ Å.

[d] Fitted constants: $\nu_0 = 17\,604.3719 \pm 0.0028$ cm^{-1}, $B_0'' = 0.090\,06 \pm 0.000\,19$ cm^{-1}, $B' = 0.067\,69 \pm 0.000\,23$ cm^{-1}, giving $r_0'' = 2.239 \pm 0.002$ Å, $r' = 2.583 \pm 0.004$ Å.

[e] This band is the most intense band we have observed, and is the 3–0 band of system D as listed in Table I.

The integrated density of states displayed in Fig. 8 for NiPd and PdPt offers an immediate explanation for the lack of an abrupt predissociation onset in these species: the number of molecular potential energy surfaces correlating to ground state atoms (or even to atomic asymptotes below 6000 cm^{-1}) is simply too small to guarantee that predissociation will occur as soon as the bond strength is exceeded. This situation is unusual for open d-shell diatomic transition metals, and is a direct consequence of the high stability of the $4d^{10}5s^0$ nondegenerate ground state of the palladium atom.

The explanation offered above for the lack of an abrupt predissociation onset in NiPd and PdPt suffers from one major drawback, particularly in the case of NiPd. It is obvious from Fig. 1 that NiPd possesses a vast number of optically accessible states in the range 15 600 to 16 600 cm^{-1}. If these states lie below the lowest dissociation threshold, then based purely upon the density of transitions in the spectrum one would expect to see an abrupt predissociation threshold further to the blue. There certainly appear to be sufficient states available for nonadiabatic perturbations to lead to predissociation. On the other hand, if the upper states observed in Fig. 1 lie above the lowest dissociation limit we are faced with another difficulty: how can a molecule excited to a region of such an obviously high density of states fail to predissociate?

The answer to this dilemma, we believe, lies again in the high stability of the $4d^{10}5s^0$, $^1S_0$ ground state of atomic palladium. In considering the chemical interaction between a $4d^{10}5s^0$, $^1S_0$ Pd atom and a $3d^94s^1$ or $3d^84s^2$ Ni atom, it seems clear that the vacant $5s$ orbital of palladium will be an excellent electron acceptor. In terms of Lewis acid–base concepts, atomic palladium is a good σ acid. Thus the initial interaction between a ground state palladium atom and either a $3d^94s^1$ or $3d^84s^2$ nickel atom will be attractive, with the $d^{10}s^0 + d^9s^1$ separated atom limit correlating to $d^{10}_{Pd}d^9_{Ni}\sigma^1$ molecular states and the $d^{10}s^0 + d^8s^2$ separated atom limit correlating to $d^{10}_{Pd}d^8_{Ni}\sigma^2$ molecular states. The lowest separated atom limit which correlates to repulsive potential energy surfaces will be the Pd d^9s^1, $^3D_3$ + Ni d^9s^1, $^3D_3$ asymptote, which lies 6769 cm^{-1} above the separated ground state atoms. Repulsive states arise from this limit when the spins of the two s electrons are triplet coupled, resulting in a $d^9_{Pd}d^9_{Ni}\sigma\sigma^*$ molecular configuration, as is certainly obtained for the quintet ($S = 2$) states arising from this limit. This situation is illustrated in Fig. 9, which presents an "artist's conception" of the electronic structure of Ni_2, NiPd, and Pd_2.

The electronic structure of Ni_2, NiPt, and Pt_2 is somewhat different than that which occurs for NiPd and PdPt. The essential difference arises because the d^9s^1, $^3D_3$ state is

TABLE III. Band systems of PdPt.[a]

System	Band[b]	ν (measured)	ν (calculated)[b]	Residual[c]
A	0–0	20 327.39	20 327.90	−0.51
	1–0	20 442.86	20 491.79	1.07
	2–0	20 557.09	20 557.23	−0.14
	3–0	20 673.34	20 674.23	−0.89
	4–0	20 793.25	20 792.78	0.47
B	0–0	20 737.96	20 737.99	−0.03
	1–0	20 849.15	20 849.07	0.08
	2–0	20 957.98	20 958.06	−0.08
	3–0	21 064.99	21 064.96	0.03
C	0–0	21 782.66	21 783.35	−0.69
	1–0	21 882.62	21 881.22	1.40
	2–0	21 979.71	21 979.27	0.44
	3–0	22 074.63	22 077.51	−2.88
	4–0	22 178.19	22 175.94	2.25
	5–0	22 274.03	22 274.56	−0.53

[a] All values are given in wave numbers. Due to uncertainty in the calibration of the dye laser used in this work, absolute band frequencies may be in error by as much as $\pm 10\ cm^{-1}$. Relative errors are probably below $\pm 2\ cm^{-1}$.

[b] Each band system was fitted to the formula $\nu = \nu_{00} + \omega'_e v' - \omega'_e x'_e (v'^2 + v')$. Assignment of the upper state vibrational numbering is probably in error in some cases, since origin bands will not always be observed due to poor Franck–Condon factors. For purposes of fitting the data the lowest frequency member observed for each progression is assigned $v' = 0$. With this procedure we obtain values of ν_{00}, ω'_e, and $\omega'_e x'_e$ as follows: System A: $\nu_{00} = 20\,327.90 \pm 1.04\ cm^{-1}$, $\omega'_e = 112.33 \pm 1.52\ cm^{-1}$, $\omega'_e x'_e = -0.78 \pm 0.30\ cm^{-1}$. System B: $\nu_{00} = 20\,737.99 \pm 0.12\ cm^{-1}$, $\omega'_e = 113.17 \pm 0.25\ cm^{-1}$, $\omega'_e x'_e = 1.05 \pm 0.06\ cm^{-1}$. System C: $\nu_{00} = 21\,783.35 \pm 2.11\ cm^{-1}$, $\omega'_e = 97.68 \pm 2.35\ cm^{-1}$, $\omega'_e x'_e = -0.09 \pm 0.38\ cm^{-1}$. The reported errors are one standard deviation in the least-squares fit.

[c] Defined as ν (measured) − ν (calculated).

the ground state of atomic platinum and the d^9s^1, $^3D_3$ state of atomic nickel lies only 204.786 cm^{-1} above the ground state. Thus the $^3D + {}^3D$ separated atom limit, which generates $d^9d^9\sigma\sigma^*$ repulsive states, lies very low in energy for Ni_2, NiPt, and Pt_2. The repulsive states correlating to this limit must slice through all of the bound states coming from higher energy asymptotes, thereby providing an efficient predissociation channel in these species. In contrast, NiPd and PdPt should possess potential energy surfaces which are more or less nested within one another, until the repulsive states originating from the $^3D_3 + {}^3D_3$ asymptote become available, which occurs at an energy over 6500 cm^{-1} above the ground state separated atoms. Therefore efficient predissociation may not occur in NiPd and PdPt until an energy is reached 6500 cm^{-1} above the lowest dissociation threshold. Subtracting this value from the energies of the highest frequency transitions observed then provides estimated bond strengths of $D_0(NiPd) \approx 1.46$ eV and $D_0(PdPt) \approx 1.98$ eV. These rough estimates of the bond strengths lead to an order of bond strengths among the platinum group dimers of $Pt_2 > NiPt > Ni_2 > PdPt > NiPd > Pd_2$, which is in agreement with the pattern of diatomic abundances observed

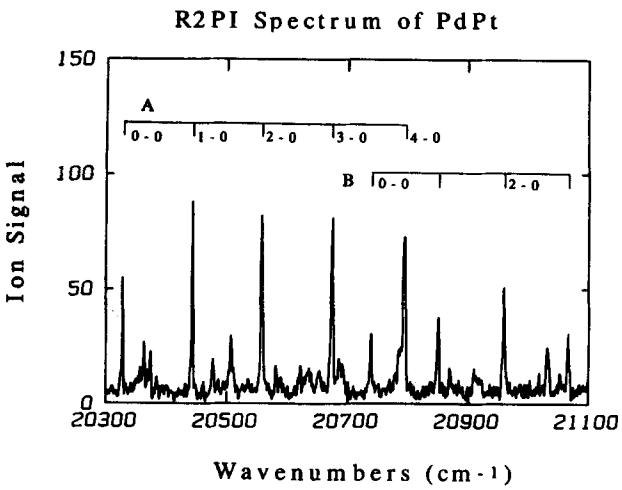

FIG. 5. Low resolution resonant two-photon ionization spectrum of PdPt, obtained using a pulsed dye laser operating on coumarin 480 in conjunction with an ArF ionization laser. The A and B band systems, as listed in Table III, are indicated on the figure.

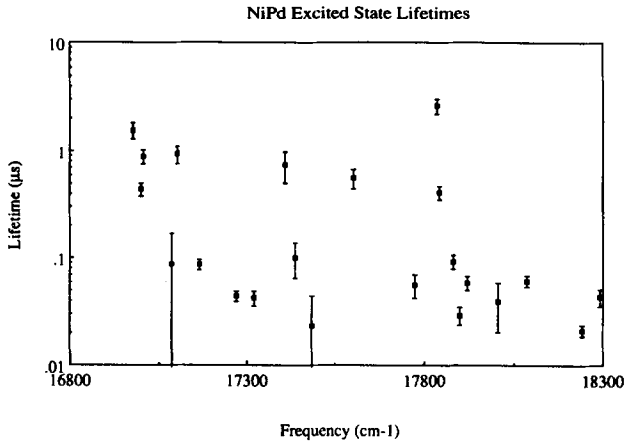

FIG. 6. Lifetimes of the excited states of NiPd, measured over the range 16 800 to 18 300 cm^{-1} by time-delayed resonant two-photon ionization methods. Although a general decrease in excited state lifetime is observed with increasing energy in this spectral range, no abrupt predissociation onset can be identified.

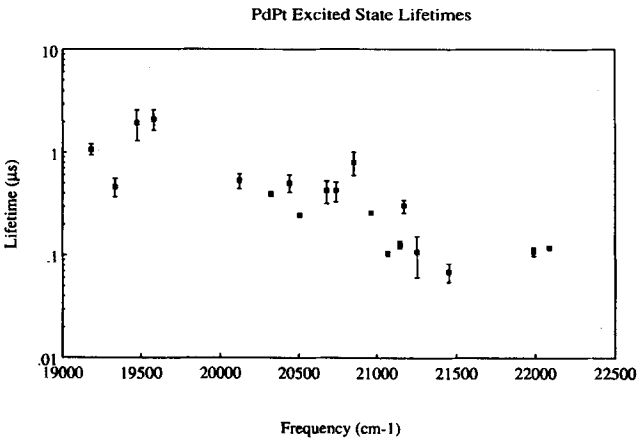

FIG. 7. Lifetimes of the excited states of PdPt, measured over the range 19 000 to 22 500 cm^{-1} by time-delayed resonant two-photon ionization methods. Again, a general decrease in excited state lifetime is observed with increasing energy, but no dramatic predissociation threshold is present.

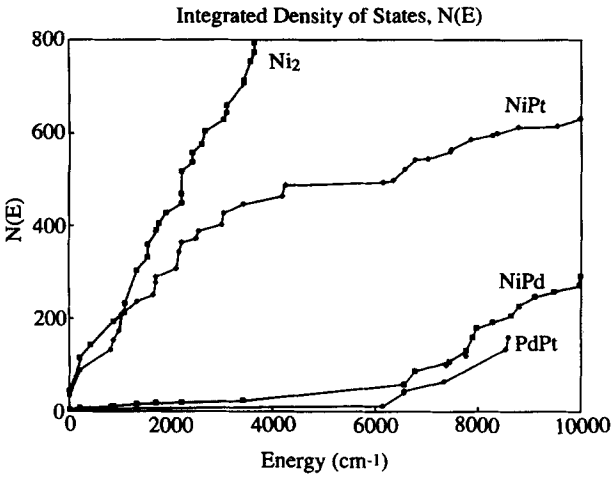

FIG. 8. Integrated density of states $N(E)$ vs E for Ni_2, NiPt, NiPd, and PdPt. In this figure $N(E)$ represents the number of distinct Hund's case (c) potential curves which arise from the interaction of two atoms with total energy between zero (ground state atoms) and E, computed using the Wigner–Witmer rules (Ref. 28) and the atomic energy levels as compiled by Moore.[9] As is evident from this figure, relatively few molecular states arise from separated atom limits below 6000 cm^{-1} for the palladium-containing species NiPd and PdPt. As discussed in Sec. IV, this relative paucity of electronic states correlating to low-lying separated atom asymptotes probably contributes to the absence of an abrupt predissociation threshold in these species.

when the equimolar NiPdPt alloy was subjected to laser vaporization.

Diatomic palladium presents a very unusual case, since the interaction of $4d^{10}5s^0$, ^1S ground state palladium atoms generates a van der Waals attraction at best. The interaction of an excited, $4d^95s^1$ Pd atom with a ground state, $4d^{10}5s^0$ atom is chemically more favorable. This combination produces a state with a σ-bond order of 1/2, but 6564 cm^{-1} of energy are required to promote the palladium atom to the $4d^95s^1$ state. As a result, the net bond strength is reduced by 6564 cm^{-1} from what it would have been if promotion of one Pd atom had not been necessary. Likewise, interaction of two $4d^95s^1$ excited palladium atoms generates a σ-bond order of 1 and likely results in some $4d$ bonding as well. Unfortunately this favorable bonding scenario comes with a promotion energy price of 13 128 cm^{-1}. Even if the intrinsic bond strength associated with bonding of two $4d^95s^1$ excited palladium atoms were as great as the bond strength of Pt_2 [$D_0(Pt_2) = 3.14 \pm 0.02$ eV],[18] the *net* bond strength of Pd_2 would be reduced by 13 128 cm^{-1} to a value of 1.51 eV. Thus the low bond strength of Pd_2 is also a direct consequence of the high stability of the $4d^{10}5s^0$, ^1S ground state of atomic palladium.

This work completes the initial survey of the chemical bonding in the platinum group dimers, as studied by resonant two-photon ionization methods. A summary of our knowledge of these species and the analogous coinage metal diatomics is provided in Table IV. It is interesting to note that although the $3d$ series diatomics Ni_2 and Cu_2 exhibit nearly identical bond lengths and bond strengths, indicating very similar bonding in these species, this similarity between the platinum group and coinage group metals does not extend to any of the other pairs of diatomic metals in this table. As judged by the criterion of bond length, significant d-orbital participation in the chemical bond is beginning to occur even in NiPd, which has a bond length 0.13 Å shorter than its coinage metal analog, CuAg.[21] As discussed in the previous article,[19] d-orbital contributions account for 0.46 eV of the bond strength of NiPt and 0.85 eV of the bonding in Pt_2.[18,19] Based on our estimated bond strength of 1.98 eV for PdPt, it would appear that this diatomic closely parallels its coinage metal analog AgAu, for which the bond strength has been measured by high-temperature mass spectrometry to be 2.06 ± 0.10 eV.[29] This comparison cannot be correct,

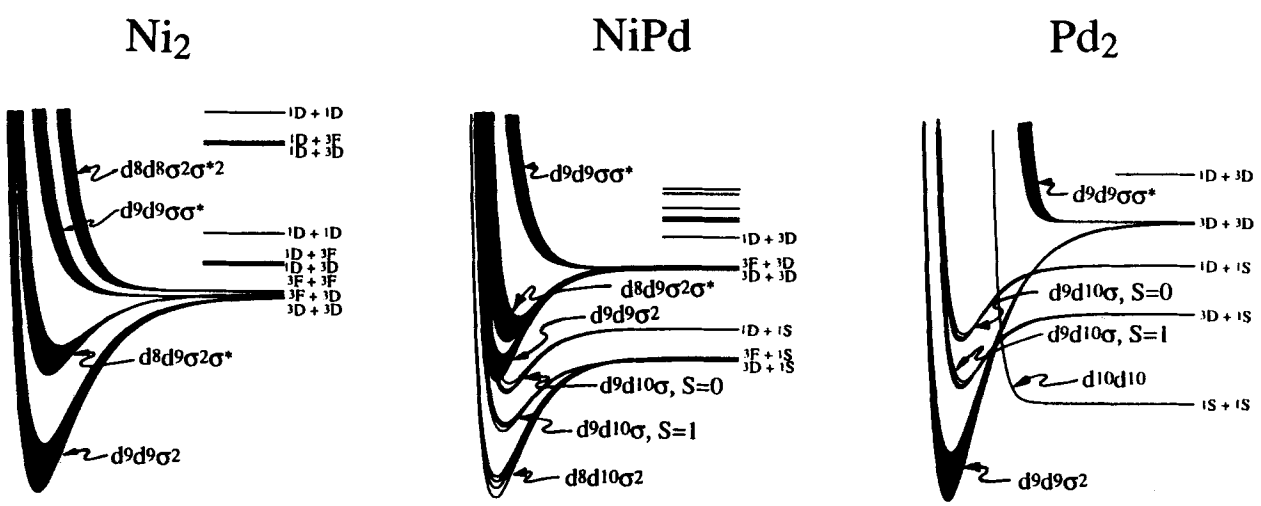

FIG. 9. Schematic diagrams of the electronic structure of Ni_2 (left), NiPd (middle), and Pd_2 (right), showing the multitudes of low-lying states arising for these species and the correlation of molecular states to the separated atom limits. The schematic potential energy curves shown for Ni_2 are representative of the Ni_2, NiPt, and Pt_2 molecules, since in all cases the lowest separated atom limit for these species is a d^9s^1, $^3D + d^9s^1$, ^3D asymptote. The diagram for NiPd is also applicable to PdPt, since in both cases all molecular states deriving from the lowest separated atom limits are expected to be bound. The situation for Pd_2 is unique, resulting in a very weak bond in this molecule. In all figures the spin–orbit splitting is omitted for simplicity.

TABLE IV. Comparison of platinum group and coinage metal dimers.

Platinum group dimer	Coinage metal dimer
Ni_2	Cu_2
$r_0 = 2.200 \pm 0.007$ Å[a]	$r_e = 2.2197$ Å[b]
$D_0 = 2.068 \pm 0.010$ eV[a]	$D_0 = 2.01 \pm 0.08$ eV[c]
$\Omega'' = 4$[a]	$^1\Sigma_g^+$ [b]
NiPd	CuAg
$r_0 = 2.242 \pm 0.005$ Å[d]	$r_0 = 2.376 \pm 0.006$ Å[e]
$D_0 < 2.27$ eV[d] ($D_0 \approx 1.46$ eV)[d]	$D_0 = 1.76 \pm 0.10$ eV[f]
$\Omega'' = 2$[d]	$^1\Sigma^+$ [e]
NiPt	CuAu
$r_0 = 2.2078 \pm 0.0023$ Å[g]	$r_e = 2.330 \pm 0.003$ Å[h]
$D_0 = 2.798 \pm 0.003$ eV[g]	$D_0 = 2.34 \pm 0.10$ eV[c,f,i]
$\Omega'' = 0$[g]	$^1\Sigma^+$ (0^+)
Pd_2	Ag_2
$r_0 = ?$	$r_0 = 2.5335 \pm 0.0001$ Å[k]
$D_0 = 1.03 \pm 0.16$ eV[j]	$D_0 = 1.65 \pm 0.03$ eV[l]
$\Omega'' = ?$	$^1\Sigma_g^+$ (0_g^+)[k]
PdPt	AgAu
$r_0 = ?$	$r_e = (2.503$ Å)[m]
$D_0 < 2.79$ eV[d] ($D_0 \approx 1.98$ eV)[d]	$D_0 = 2.06 \pm 0.10$ eV[f]
$\Omega'' = ?$	$^1\Sigma^+$ (0^+)
Pt_2	Au_2
$r_0 = ?$	$r_e = 2.4719$ Å[o]
$D_0 = 3.14 \pm 0.02$ eV[n]	$D_0 = 2.29 \pm 0.02$ eV[p]
$\Omega'' = ?$	$^1\Sigma_g^+$ (0_g^+)[o]

[a] Reference 17.
[b] Reference 31.
[c] Reference 1.
[d] This work.
[e] Reference 21.
[f] Reference 29.
[g] Reference 19.
[h] Reference 37.
[i] Reference 32.
[j] References 13 and 27.
[k] Reference 33.
[l] Reference 34.
[m] Estimated as $[r_0(Ag_2) + r_e(Au_2)]/2$.
[n] Reference 18.
[o] Reference 35.
[p] Reference 36.

however, since the palladium atom must be promoted to form a strong bond to platinum. Presumably the promotion energy required to prepare the Pd atom for bonding is compensated by d-orbital bonding contributions in PdPt. These may be nearly as large in PdPt as in Pt_2, since the $4d$ orbitals of Pd ($\langle r \rangle_{4d} = 0.8185$ Å)[30] are nearly as large as the $5d$ orbitals of Pt ($\langle r \rangle_{5d} = 0.8746$Å).[30] High-resolution studies of PdPt and AgAu are expected to confirm the importance of d-orbital contributions to the chemical bonding in PdPt by demonstrating a significantly shorter bond length in PdPt than in AgAu. Finally, the electronic structure of Pd_2 differs greatly from that of Ag_2 primarily because of the need to promote both palladium atoms to form a $5s\sigma$ bond. This results in a greatly weakened bond in Pd_2 as compared to any of the remaining platinum group or coinage metal diatomics.

V. CONCLUSION

Resonant two-photon ionization spectroscopy of jet-cooled NiPd and PdPt has been used to investigate the chemical bonding in these species. A dense spectrum has been found for NiPd over the range 12 150 to 18 300 cm^{-1}, and four vibrational progressions have been assigned. High resolution studies are reported for three vibronic bands, resulting in an assignment of the ground state of $^{58}Ni^{105}Pd$ as an $\Omega'' = 2$ state with $B_0'' = 0.089\,83 \pm 0.0004$ cm^{-1} ($r_0'' = 2.242 \pm 0.005$ Å). The molecule expands upon electronic excitation in the three bands investigated, giving values of r' for the upper states ranging between 2.506 and 2.583 Å.

The spectrum obtained for PdPt is far less dense than that found for NiPd, probably indicating a greater degree of d-orbital interactions in this species. Three vibronic progressions have been identified, with upper state vibrational frequencies in the range from 97 to 113 cm^{-1}. The observed vibronic bands, along with the ionization frequencies used to observe them, bracket the ionization potential as IP(NiPd) $= 7.18 \pm 0.76$ eV and IP(PdPt) $= 8.27 \pm 0.38$ eV. Despite a careful search over the range 11 375 to 23 000 cm^{-1}, no spectroscopic transitions have been observed in Pd_2 at all. This confirms that Pd_2 possesses a weak bond, with $D_0(Pd_2) < 1.41$ eV, in agreement with the results of high temperature mass spectrometry.

In contrast to the results obtained for Ni_2,[17] NiPt,[19] and Pt_2,[18] neither NiPd nor PdPt exhibits an abrupt predissociation threshold. As a result it has been impossible to provide an accurate measurement of the bond strength in these species. Assuming predissociation sets in promptly at the first separated atom limit which generates repulsive potential energy curves, however, we estimate the bond strengths as $D_0(NiPd) \approx 1.46$ eV and $D_0(PdPt) \approx 1.98$ eV. These values are only very approximate, but they are consistent with the abundances of diatomic species produced when an equimolar alloy of NiPdPt is vaporized. They are also consistent with the promotion energy required to prepare atomic palladium for chemical bonding and the expected degree of d-orbital contributions to the bond strength (as estimated from results on Ni_2,[17] NiPt,[19] and Pt_2[18]).

Finally, the platinum group dimers have been compared to the diatomic coinage metals. Apart from Ni_2/Cu_2, these two groups of diatomic metals have little in common. The unique stability of the $4d^{10}5s^0$, ^1S ground state of palladium results in a dramatic weakening of the metal–metal bond in palladium-containing diatomics, and the propensity for formation of significant d-electron bonds in platinum compounds greatly stabilizes the platinum-containing diatomics as compared to their coinage metal analog.

ACKNOWLEDGMENTS

We are grateful to Professor William H. Breckenridge for the use of the intracavity etalon and accessories employed in the high resolution investigations. Jeff Bright is thanked for his expert help in preparing the NiPd sample. We also gratefully acknowledge research support from the National Science Foundation under Grant Nos. CHE-85-21050 and CHE-89-12673. Acknowledgment is also made to the donars of the Petroleum Research Fund, administered by the American Chemical Society, for partial support of this research.

[1] M. D. Morse, Chem. Rev. 86, 1049 (1986).
[2] D. J. Trevor and A. Kaldor, ACS Symp. Ser. 333, 43 (1987).

[3]W. Weltner, Jr. and R. J. Van Zee, Annu. Rev. Phys. Chem. **35**, 291 (1984).
[4]A. Kaldor, D. M. Cox, and M. R. Zakin, Adv. Chem. Phys. **70**, 211 (1988).
[5]S. R. Langhoff and C. W. Bauschlicher, Jr., Annu. Rev. Phys. Chem. **39**, 181 (1988).
[6]D. R. Salahub, Adv. Chem. Phys. **69**, 447 (1987).
[7]I. Shim, Mat.-Fys. Meddr. Danske Vidensk. Selsk. (16 Res. Rep. of Niels Bohr Fellows) **41**, 147 (1985).
[8]J. Koutecky and P. Fantucci, Chem. Rev. **86**, 539 (1986).
[9]C. E. Moore, Natl. Bur. Stand. Circ. No. 467 (1971), Vols. II and III.
[10]T. H. Upton and W. A. Goddard, III, J. Am. Chem. Soc. **100**, 5659 (1978).
[11]I. Shim, J. P. Dahl, and H. Johansen, Int. J. Quantum Chem. **15**, 311 (1979).
[12]J. O. Noell, M. D. Newton, P. J. Hay, R. L. Martin, and F. W. Bobrowicz, J. Chem. Phys. **73**, 2360 (1980).
[13]I. Shim and K. A. Gingerich, J. Chem. Phys. **80**, 5107 (1984).
[14]K. Balasubramanian, J. Chem. Phys. **89**, 6310 (1988).
[15]H. Basch, D. Cohen, and S. Topiol, Isr. J. Chem. **19**, 233 (1980).
[16]K. Balasubramanian, J. Chem. Phys. **87**, 6573 (1987).
[17]M. D. Morse, G. P. Hansen, P. R. R. Langridge-Smith, L.-S. Zheng, M. E. Geusic, D. L. Michalopoulos, and R. E. Smalley, J. Chem. Phys. **80**, 5400 (1984).
[18]S. Taylor, G. W. Lemire, Y. Hamrick, Z. -W. Fu, and M. D. Morse, J. Chem. Phys. **89**, 5517 (1988).
[19]S. Taylor, E. M. Spain, and M. D. Morse, J. Chem. Phys. **92**, 2698 (1990).
[20]Z. -W. Fu and M. D. Morse, J. Chem. Phys. **90**, 3417 (1989).
[21]G. A. Bishea, N. Marak, and M. D. Morse (in preparation).
[22]Z. -W. Fu, G. W. Lemire, Y. Hamrick, S. Taylor, J. -C. Shui, and M. D. Morse, J. Chem. Phys. **88**, 3524 (1988).
[23]S. Gerstenkorn and P. Luc, *Atlas du Spectre d'Absorption de la Molécule d'Iode* (CNRS, Paris, France, 1978).
[24]S. Gerstenkorn and P. Luc, Rev. Phys. Appl. **14**, 791 (1979).
[25]S. C. O'Brien, Y. Liu, Q. Zhang, J. R. Heath, F. K. Tittel, R. F. Curl, and R. E. Smalley, J. Chem. Phys. **84**, 4074 (1986).
[26]D. R. Stull and G. C. Sinke, *Thermodynamic Properties of the Elements, Advances in Chemistry Series 18* (American Chemical Society, Washington, D. C., 1956).
[27]S. -S. Lin, B. Strauss, and A. Kant, J. Chem. Phys. **51**, 2282 (1969).
[28]G. Herzberg, *Molecular Spectra and Molecular Structure. I. Spectra of Diatomic Molecules*, 2nd ed. (Van Nostrand Reinhold, New York, 1950), pp. 315–322.
[29]M. Ackerman, F. E. Stafford, and J. Drowart, J. Chem. Phys. **33**, 1784 (1960).
[30]J. P. Desclaux, At. Data Nucl. Data **12**, 311 (1973).
[31]N. Aslund, R. F. Barrow, W. G. Richards, and D. N. Travis, Ark. Fys. **30**, 171 (1965).
[32]J. E. Kingcade, U. V. Choudary, and K. A. Gingerich, Inorg. Chem. **18**, 3094 (1979).
[33]B. Simard, P. A. Hackett, A. M. James, and P. R. R. Langridge-Smith (in preparation).
[34]K. Hilpert and K. A. Gingerich, Ber. Bunsenges. Phys. Chem. **84**, 739 (1980).
[35]L. L. Ames and R. F. Barrow, Trans. Faraday Soc. **63**, 39 (1967).
[36]J. Kordis, K. A. Gingerich, and R. J. Seyse, J. Chem. Phys. **61**, 5114 (1974).
[37]G. A. Bishea, J. C. Pinegar, and M. D. Morse (in preparation).